# Arctic greening associated with lengthening growing seasons in Northern Alaska

Arndt, Kyle A ; Santos, Maria J ; Ustin, Susan ; Davidson, Scott J ; Stow, Doug ; Oechel, Walter C ; Tran, Thao T P ; Graybill, Brian ; Zona, Donatella

Abstract: Many studies have reported that the Arctic is greening; however, we lack an understanding of the detailed patterns and processes that are leading to this observed greening. The normalized difference vegetation index (NDVI) is used to quantify greening, which has had largely positive trends over the last few decades using low spatial resolution satellite imagery such as AVHRR or MODIS over the pan-Arctic region. However, substantial fine scale spatial heterogeneity in the Arctic makes this large-scale investigation hard to interpret in terms of vegetation and other environmental changes. Here we focus on one area of the northern Alaskan Arctic using high spatial resolution (4 m) multispectral satellite imagery from DigitalGlobe™ to analyze the greening trend near Utqiaġvik (formerly known as Barrow) over 14 years from 2002 to 2016. We found that tundra vegetation has been greening ( = 0.65, p = 0.01, NDVI increase of 0.01 yr−1) despite no overall change in vegetation community composition. The greening is most closely correlated to the number of thawing degree days (R 2 = 0.77, F = 21.5, p < 0.001) which increased in a similar linear trend over the 14 year study period (1.79 ± 0.50 days per year, p < 0.01, = −0.56). This suggests that in this Arctic ecosystem, greening is occurring due to a lengthening growing season that appears to stimulate plant productivity without any significant change in vegetation communities. We found that vegetation communities in wetter locations greened about twice as fast as those found in drier conditions supporting the hypothesis that these communities respond more strongly to warming. We suggest that in Arctic environments, vegetation productivity may continue to rise, particularly in wet areas.

DOI: https://doi.org/10.1088/1748-9326/ab5e26

DOI: https://doi.org/10.1088/1748-9326/ab5e26

# Arctic greening associated with lengthening growing seasons in Northern Alaska

To cite this article before publication: Kyle Arndt *et al* 2019 *Environ. Res. Lett.* in press https://doi.org/10.1088/1748-9326/ab5e26

# Arctic Greening Associated with Lengthening Growing Seasons in Northern Alaska

Kyle A. Arndt[1,2], Maria J. Santos[3], Susan Ustin[2], Scott J. Davidson[4], Doug Stow[5], Walter C. Oechel[1,6], Thao T. P. Tran[7], Brian Graybill[1], and Donatella Zona[1,8]

[1] *Biology Department, San Diego State University, San Diego, USA*
[2] *Department of Land, Air and Water Resources, University of California at Davis, Davis, USA*
[3] *Department of Geography, University of Zurich, Zurich, CH*
[4] *Department of Geography and Environmental Management, University of Waterloo, Waterloo, CA*
[5] *Department of Geography, San Diego State University, San Diego, USA*
[6] *Department of Geography, College of Life and Environmental Sciences, University of Exeter, Exeter, UK*
[7] *Department of Earth and Planetary Science, University of California Berkeley, Berkeley, CA*
[8] *Department of Animal and Plant Sciences, University of Sheffield, Sheffield, UK*

E-mail: karndt-w@sdsu.edu

## Abstract

Many studies have reported that the Arctic is greening; however, we lack an understanding of the detailed patterns and processes that are leading to this observed greening. The normalized difference vegetation index (NDVI) is used to quantify greening, which has had largely positive trends over the last few decades using low spatial resolution satellite imagery such as AVHRR or MODIS over the pan-Arctic region. However, substantial fine scale spatial heterogeneity in the Arctic makes this large-scale investigation hard to interpret in terms of vegetation and other environmental changes. Here we focus on one area of the northern Alaska Arctic using high spatial resolution (4 m) multispectral satellite imagery from DigitalGlobe™ to analyze the greening trend near Utqiaġvik (formerly known as Barrow), Alaska over 14 years from 2002 to 2016. We found that tundra vegetation has been greening ($\tau = 0.65$, $p = 0.01$, NDVI increase of 0.01 $yr^{-1}$) despite no overall change in vegetation community composition. The greening is most closely correlated to the number of thawing degree days ($R^2 = 0.77$, $F = 21.5$, $p < 0.001$) which, increased in a similar linear trend over the 14-year study period ($1.79 \pm 0.50$ days per year, $p < 0.01$, $\tau = -0.56$). This suggests that in this Arctic ecosystem, greening is occurring due to a lengthening growing season that appears to stimulate plant productivity without any significant change in vegetation communities. We found that vegetation communities in wetter locations greened about twice as fast as those found in drier conditions supporting the hypothesis that these communities respond more strongly to warming. We suggest that in Arctic environments, vegetation productivity may continue to rise, particularly in wet areas.

Keywords: High-Resolution, Arctic Greening, Remote Sensing, Time-series, Warming

## 1. Introduction

Vegetation trends are important to the carbon balance of Arctic ecosystems (Joos et al., 2001, Mishra and Riley, 2012). Organic carbon content in Arctic soils is about 1,300 Pg (Hugelius et al., 2014); roughly twice the current total atmospheric carbon content (IPCC, 2013). Accelerated

warming is occurring in the Arctic as a result of climate change and positive feedbacks (IPCC, 2013, Chapin et al., 2005, Serreze and Francis, 2006) putting this large carbon pool at risk of loss to the atmosphere (Schuur et al., 2013, Schuur et al., 2015). Increasing permafrost temperatures (Romanovsky et al., 2017), lateral flow of organic matter (Spencer et al., 2015), and disturbance (Price et al., 2013) are contributing to carbon losses. Carbon exchanges vary between wet and dry vegetation communities where wet communities (often standing water dominated by wetland sedges) are typically characterized by strong uptake of carbon dioxide ($CO_2$) (Sturtevant and Oechel, 2013, Treat et al., 2018) and strong methane ($CH_4$) emissions (Davidson et al., 2016b, Treat et al., 2018). Dry communities (dominated by mosses, lichens and shrubs with a sub-surface water table) typically exhibit weaker uptake or sometimes net release of $CO_2$ and low emissions of $CH_4$ (Treat et al., 2018, Natali et al., 2015).

Changes in vegetation productivity have been measured by monitoring the normalized difference vegetation index (NDVI) calculated from satellite imagery (Bhatt et al., 2010, Goetz et al., 2005, Jia et al., 2003). NDVI is positively correlated to vegetation biomass across Arctic tundra biomes (Jia et al., 2003, Epstein et al., 2012, Raynolds et al., 2011) therefore NDVI increases are defined as "greening" and NDVI decreases are defined as "browning". Researchers have detected greening trends across the pan-Arctic over the past several decades (Bhatt et al., 2010, Bhatt et al., 2014, Jia et al., 2003); however, greening trends have started to weaken (Piao et al., 2014) or reverse with large browning areas, specifically in the European Arctic and Seward Peninsula (Bhatt et al., 2013, Bhatt et al., 2017, Lara et al., 2018, Phoenix and Bjerke, 2016).

Greening has predominantly been attributed to large-scale climate conditions including rising temperatures linked to reduced albedo over the ocean due to sea ice decline (Bhatt et al., 2010, Bhatt et al., 2014, Macias-Fauria et al., 2017). In lower latitude Arctic regions, greening has been associated with shrub encroachment (Forbes et al., 2010, Myers-Smith et al., 2011, Tape et al., 2006), which also has a positive feedback with warming (Chapin et al., 2005). Greening has also been correlated to shifting moisture regimes (Bhatt et al., 2017, Westergaard-Nielsen et al., 2017) and increases in temperature and precipitation due to movements of air masses from lower latitudes (Macias-Fauria et al., 2017).

Most studies on Arctic greening use coarse satellite imagery including AVHRR and MODIS with spatial resolutions of 1-8 km and 0.25-1 km, respectively. These images provide broad coverage of the pan-Arctic, are relatively continuous temporally, and are useful for determining global trends. However, due to the coarse spatial resolution, fine details of patterns and processes are indiscernible and has limited our understanding of greening and browning (Bartsch et al., 2016, Myers-Smith et al., 2019), particularly in ecosystems characterized by fine spatial heterogeneity such as Arctic tundra (Billings and Peterson, 1980, Webber, 1978)

Recent studies have taken more detailed approaches to assess greening in the Arctic by utilizing Landsat satellites (30 m spatial resolution) (Frost et al., 2014, Lara et al., 2018, Nitze and Grosse, 2016, Raynolds and Walker, 2016). Some studies found that browning can be muddled by surface water due to the strong absorption radiance by water despite greening of vegetation (Raynolds and Walker, 2016). Others have shown how the heterogeneity of vegetation cover, geomorphic landscape type, and climate regimes can impact the rate and trend of greening (Lara

et al., 2018). While Landsat's 30 m spatial resolution is able to cover a large spatio-temporal extent, it does not fully capture the heterogeneity within Arctic ecosystems, which have fine scale polygonal landforms often less than 30 m across (Billings and Peterson, 1980, Webber, 1978).

Here we present a high spatial resolution (4 m) analysis of greening for an area near Utqiaġvik (formerly Barrow), Alaska. As more high spatial resolution satellite imagery is collected, these time-series approaches will become increasingly valuable (Stow et al., 2004) and offer new opportunities and challenges for studying these complex, heterogeneous ecosystems. These tools and their results will likely prove beneficial for modeling carbon dynamics over multiple scales and validating trends reported by larger scales studies. In our study, we aim to (1) show if vegetation communities have changed, (2) analyze fine-scale spatial NDVI trends, and (3) assess correlates of shifts in vegetation communities and NDVI.

## 2. Methodology

### 2.1 Study Area

Our study was conducted on the Barrow Environmental Observatory (BEO) located near Utqiaġvik, Alaska (***Figure 1***). The BEO has a long research history, resulting in a high frequency of satellite tasking, a relatively steady meteorological data record, and accessible field sites. Located in the Arctic Coastal Plain, the site is on continuous permafrost and consists of several drained lake basins (hereby basins), differing in time since drainage (Hinkel et al., 2003), and ice-wedge polygon formations due to a seasonal freeze-thaw cycle (Webber, 1978). Dominant vegetation in the region is characterized as a sedge/grass moss wetland (Walker et al., 2005). Further details are available in the supplementary material.

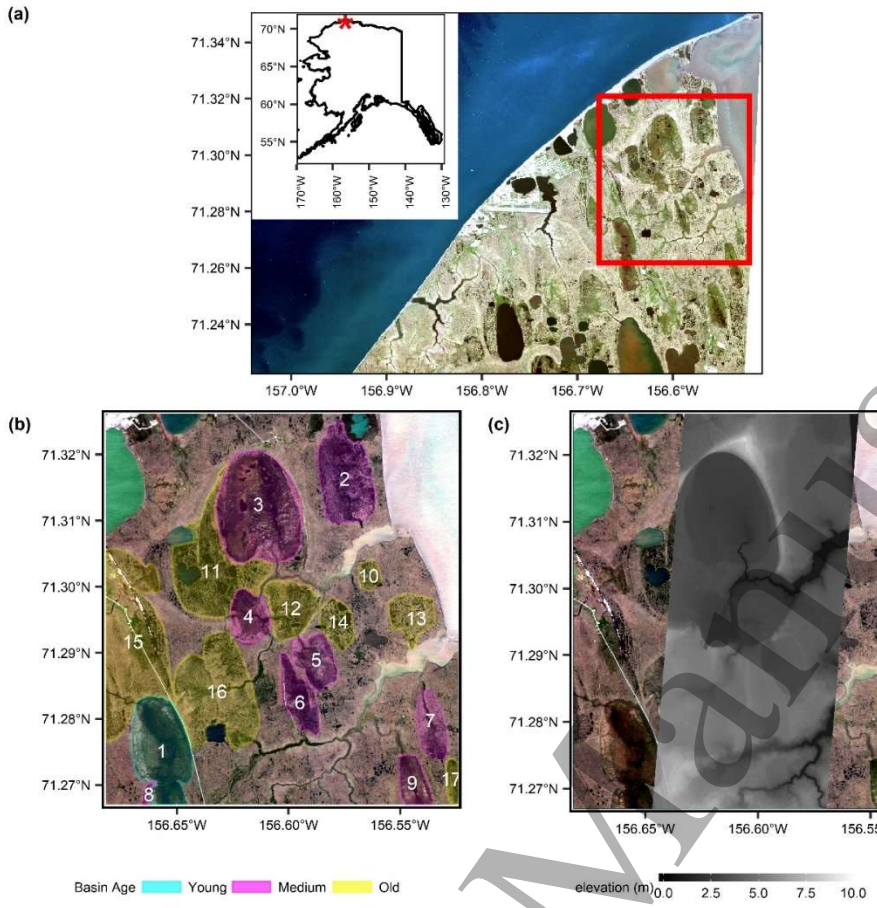


***Figure 1:*** **(a)** An overview of the study area showing the location of Utqiaġvik in Alaska represented by a red star. The study area extent is highlighted with a red box in the true color RGB mosaic acquired 22 July 2015 by WV2. **(b)** Basins over the study area; colors represent the age of basins according to Hinkel et al. (2003). The blue is the only young age basin in the study area (basin 1). There were eight medium age basins (purple) and eight old basins (yellow). Basin numbers are labelled according to age and then generally north to south. **(c)** Digital elevation model coverage through the study area. There is a gentle slope from the southern extent to the north with tributaries to the Elson Lagoon and basins as the lowest parts across the landscape. The background of panels b and c are a true-color RGB image taken 24 July 2016 by WV3.

## 2.2 Imagery data acquisition and pre-processing

Imagery used in this study was procured through the Polar Geospatial Center at the University of Minnesota (***Table 1***). Acquisition dates spanned 14 years, with the earliest Ikonos image acquired 18, July 2002 and the final WorldView-3 image acquired 24, July 2016. A digital elevation model (***Figure 1b***) was used to measure the relative elevation of features (Wilson et al., 2013). The largest overlapping area in all images defined the study area extent with the northwest corner at 71°19’34.36” N, 156°41’20.62” W and the southeast corner at 71°16'9.02" N, 156°31'26.44" W. The total study area was 37.42 km$^2$. Supplementary materials provide details on image pre-processing.

***Table 1***: Inventory of the images used for the study including the acquisition date of the image and the sensor used. All imagery used were DigitalGlobe™ assets (© Maxar Technologies, USA). Sensors are as follows: IKO, Ikonos;

QB2, QuickBird-2; WV2, WorldView-2; WV3, WorldView-3. July and August images were used in time-series analysis.

| Acquisition Date | Sensor |
|---|---|
| 18-Jul-02 | IKO |
| 02-Aug-02 | QB2 |
| 16-Jun-06 | QB2 |
| 21-Jul-10 | WV2 |
| 24-Jul-10 | WV2 |
| 25-Jul-10 | WV2 |
| 03-Aug-10 | WV2 |
| 10-Jul-11 | WV2 |
| 05-Jul-12 | WV2 |
| 13-Aug-12 | WV2 |
| 30-Jun-14 | WV2 |
| 24-Jun-15 | WV2 |
| 22-Jul-15 | WV2 |
| 20-Jul-16 | WV2 |
| 24-Jul-16 | WV3 |

*2.2.1 Meteorological data*

Hourly air temperature and relative humidity data from the Barrow Atmospheric Baseline Observatory (BRW, NOAA), located north of the study area (71.3230 °N, 156.6114 °W), were used to understand climatic conditions during growing seasons. Mean growing season (June - August) air temperature, vapor pressure deficit (VPD), growing degree days (GDD, cumulative mean daily air temperatures over 0 °C), and thawing degree days (TDD, cumulative days with a mean air temperature over 0 °C) were calculated. TDD and GDD were calculated for image acquisition dates allowing NDVI comparisons.

## 2.3 Field data collection

Field surveys were conducted in July 2018. Eight transects were surveyed with a total of 297 1 m x 1 m plots. Transects ranged from 100 to 300 meters in length and plots were surveyed every 5 m. For each plot, plant types (grass, moss, lichen, shrub, open water, and forb), thaw depth, soil moisture, and canopy height were measured (see supplementary materials for descriptions of field techniques). Medians and standard deviations are reported as summary statistics. Coordinates of plots were recorded using a Trimble 5700 differential global positioning system (Trimble®, USA).

## 2.4 Random forest vegetation model

Pixels with NDVI value below 0.1 (Gandhi et al., 2015) were masked to remove snow and water, which have extremely high or low reflectance. Then we used histogram matching to color correct images with the 2016 WorldView-3 image as the base (results in supplementary material). Bright and dark objects were removed by the NDVI filter, therefore these objects will not skew histograms and allow for a better comparison of illumination. A tasseled cap transformation was

done to produce three orthogonal polynomial combinations representing brightness, wetness, and greenness of objects (Kauth and Thomas, 1976, Yarbrough et al., 2005).

Vegetation community classes from "wet" and "dry" locations were chosen based on functional relationships with carbon cycling (Sturtevant and Oechel, 2013, Treat et al., 2018, Davidson et al., 2016b, Natali et al., 2015) and being spectrally separable. An additional open water class was included after vegetation classification; corresponding to pixels removed by the NDVI filter. We utilized a random forest machine learning algorithm for the vegetation classification model because of its high accuracy when predicting vegetation classes (Chapman et al., 2009, van Beijma et al., 2014). Four spectral bands (blue, green, red, and near-infrared (NIR)) and three tasseled cap variables were used to train the random forest model. Welch two sample t-tests were used to test for significant differences in spectral properties between vegetation communities (see supplementary material). The random forest model was then applied to all 15 images for predicting vegetation communities. Model accuracy was assessed using 30% of ground reference points not used in model training, against the classification of the latest 24, July 2016 WorldView-3 image.

### 2.5 Greening assessment

Greening of vegetation was measured using NDVI following many Arctic studies (Bhatt et al., 2013, Bhatt et al., 2010, Epstein et al., 2012). Changes in NDVI were estimated prior to applying the NDVI threshold and histogram matching, since open water can contribute to browning (Raynolds and Walker, 2016) which, we wanted to allow. Since NDVI changes most rapidly during green-up (Zhang et al., 2018), differs seasonally and saturates (Suzuki et al., 2001), only peak season (mid-July to early August) image acquisitions were used in the time-series analysis. This approach captured NDVI shifts linked to long term changes instead of seasonal differences due to acquisition dates. We also calculated a pixel level change to locate finely detailed space-time anomalies by regressing each pixel's NDVI over time.

### 2.6 Statistical analyses

Non-metric multidimensional scaling (NMDS) was used to determine ecological separability between vegetation communities using the "vegan" package (Oksanen et al., 2018). Differences in the physical environmental parameters were determined using Welch two sample t-tests; the t-statistic (t), degrees of freedom (df), and p-value ($p$) are reported for these tests. Homogeneity of variance was tested for all parameters before significance testing.

Changes in vegetation coverage, NDVI, and TDD over time were calculated according to Yue et al. (2002) using the "zyp" package (Bronaugh and Werner, 2019), which is sensitive to potential autocorrelation in time-series data. These changes were analyzed over the entire image and by separating the landscape into the following age based categories of basins (Hinkel et al., 2003): young basins (0-50 years old), medium basins (50-300 years old), old basins (300-2000 years old), and the "other" category that accounts for the remaining landscape (***Figure 1a***). Before analyzing controls on NDVI, data were detrended to avoid temporal autocorrelation by taking the residuals of the least squares linear model between year and the given variable.

NDVI controls were analyzed using linear mixed effects models (LMEs) using maximum likelihood in the "nlme" package (Pinheiro et al., 2018) and the "MuMIn" package (Barton, 2018) was used to calculate the coefficient of determination of these LMEs. Two components of coefficients of determination are reported for each LME, marginal ($R^2_m$) and conditional ($R^2_c$), representing the coefficient of fixed effects and full model respectively. LMEs were compared to a null model with only year as a temporal random effect using analysis of variance. LMEs included single variable models with each variable as fixed variables (GDD, TDD, mean air temperature, and mean VPD) and a full multivariate model with TDD, mean air temperature, and mean VPD.

To determine pixel level greening and browning trends, the Theil-Sen slope method (Sen, 1968, Theil, 1992) was used for the rate of change and Yue et al. (2002) time-series methods were again used to determine statistical significance. This method of trend detection performs better in remote sensing data than more basic least-squares regression (Fernandes and Leblanc, 2005). NDVI of each pixel over time was regressed using the "spatialEco" package (Evans, 2018), resulting in rasters of Kendall's τ statistics (ranging from -1 to 1 with values closer to 0 indicating no significant trend) and Theil-Sen slope. All statistical analyses were conducted using R v.3.5.2 statistical software (R Core Team, 2018).

## 3. Results

### 3.1 Vegetation community differentiation

Vegetation communities were separable with NMDS showing distinct communities based on vegetation composition (***Figure 2a***), and environmental conditions (***Figure 2 b-d***). Soil moisture was 55.09 ± 12.40% and 83.18 ± 3.33% for dry and wet communities respectively, and significantly different (t = -23.4, df = 143.6, $p < 0.001$, ***Figure 2b***). Canopy heights were also significantly different (t = -11.7, df = 280.4, $p < 0.001$, ***Figure 2c***), with higher wet than dry vegetation (19 ± 8.99 cm and 10 ± 5.49 cm, respectively). Thaw depths were not significantly different between communities with depths of 24.0 ± 7.2 cm and 24.7 ± 7.9 cm for dry and wet communities (t = -0.93, df = 287.8, $p = 0.35$, ***Figure 2d***).

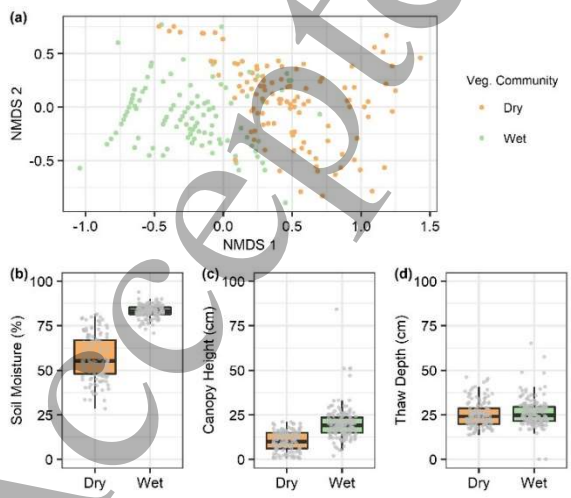

***Figure 2***: **(a)** Non-metric multidimensional scaling (NMDS) components 1 and 2 show ecologically unique vegetation communities of dry and wet vegetation communities shown by sample clustering. **(b)** Soil moisture is significantly different between the dry and wet vegetation (t = -23.4, df = 143.6, $p < 0.001$). **(c)** Canopy height is also significantly different between vegetation classes (t = -11.7, df = 280.4, $p < 0.001$), wet communities having higher growth. **(d)** Thaw depth is not significantly different between communities (t = -0.93, df = 287.8, $p > 0.05$).

### 3.2 Vegetation classification

The random forest vegetation classification had 82% overall accuracy. Producer's accuracy was slightly higher for wet communities (86%) than dry communities (78%) and user's accuracy was comparable for wet (83%) and dry (82%) communities. Twenty-five bootstrapped repetitions of the training data for random forest model yielded an overall accuracy of 89%.

Change detection between imagery dates revealed negligible change in the overall areal extent of vegetation communities from 2002 to 2016. There was about a half percent loss of dry community area (16 ha) corresponding mostly to gains in open water (15 ha) and a small increase in the wet community (1 ha), in line with errors in areal estimates stemming from image classification. A 2002 to 2016 change map (***Figure 3***) showed spatial trends of wetter areas becoming wetter and drier areas becoming drier which, appear relatively balanced from the total analysis.

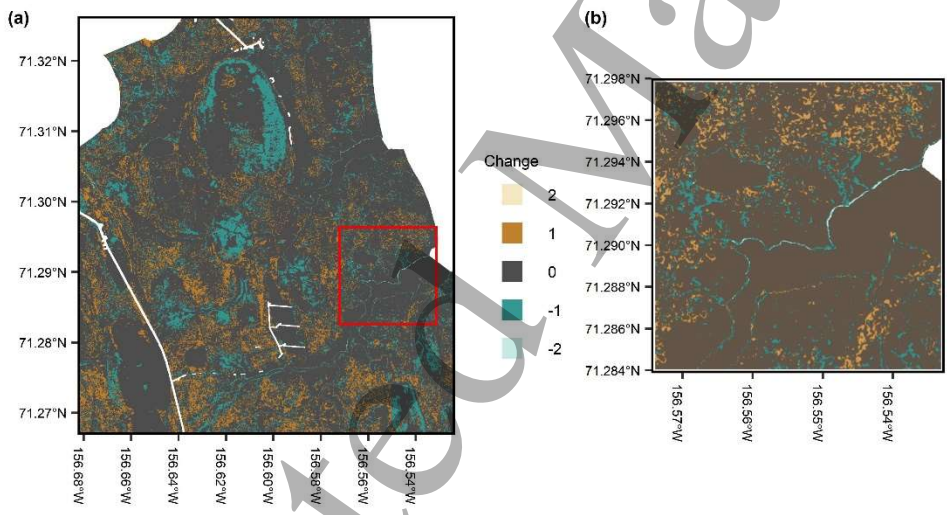


***Figure 3:*** Change map of the vegetation community changes from 2002 to 2016. Numbers represent the magnitude of change with brown changes representing changes to drier communities and blue green to wetter. A positive two would be a change from open water to dry and a negative two from dry to open water. White areas are anthropogenic areas that were masked for all analyses. **(a)** The entire study area where it appears that wetter areas became wetter and dry areas became drier which ultimately balanced out over the landscape. **(b)** An enlarged subset of the red rectangle seen in panel ***a*** that shows dry community to open water changes showing possible erosion along the larger tributaries leading to the Elson lagoon. The edges of larger open water seemed to transition to wet vegetation or open water.

#### *3.2.1 Vegetation composition by basin age*

There was no noticeable change in vegetation community composition in the young basin with overall changes less than 1% (< 1 ha). Medium age basins by contrast showed a 16% increase in wet communities (85 ha) corresponding to similar losses in dry communities. Old basins had a

4% decrease in wet communities (26 ha) and similar increase in dry communities (24 ha). The remainder of the landscape showed little change with wet communities decreasing by 3% and dry communities increasing by the same amount. The only significant trend was open water in the "other" landscape area ($\tau = 0.77$, $p = 0.002$, slope = 0.72 ha/year). All other trends were not significant.

*3.2.2 Vegetation change at individual basins*

Some significant trends in vegetation cover were observed within specific basins (***Table 2***). Three medium age basins (3, 4 and 5) had significant increases in wet communities which, corresponded to losses in dry communities. Conversely, old basin number 10 gained dry community area but had no clear reciprocal change in open water or wet communities. Since there was only one young basin, these results do not differ from above finding no significant change.

***Table 2:*** Time-series statistics for each individual basin with regards to the NDVI and vegetation communities. Units for the vegetation communities are in hectares. The *p*-value is derived from Kendall's Tau and the slope is derived from Theil-Sen.

| | | Dry | | | Wet | | | Water | | | NDVI | | |
|---|---|---|---|---|---|---|---|---|---|---|---|---|---|
| Basin Number | Basin Age | *p*-value | Tau | Slope | *p*-value | Tau | Slope | *p*-value | Tau | Slope | *p*-value | Tau | Slope |
| 1 | Young | 0.421 | 0.216 | 0.223 | 0.334 | -0.256 | -0.216 | 1.000 | 0.198 | -0.365 | 0.077 | 0.452 | 0.009 |
| 2 | Medium | 0.053 | 0.492 | 0.438 | 0.077 | -0.452 | -0.419 | 0.629 | -0.138 | 0.050 | **0.016** | 0.610 | 0.013 |
| 3 | Medium | **0.036** | -0.531 | -2.931 | **0.036** | 0.531 | 2.846 | **0.006** | 0.688 | 0.039 | **0.024** | 0.570 | 0.013 |
| 4 | Medium | **0.016** | -0.610 | -1.125 | **0.016** | 0.610 | 1.125 | 1.000 | 0.000 | -0.002 | **0.010** | 0.649 | 0.014 |
| 5 | Medium | **0.036** | -0.531 | -0.627 | **0.036** | 0.531 | 0.627 | N/A | N/A | N/A | **0.006** | 0.688 | 0.015 |
| 6 | Medium | 1.000 | 0.198 | -0.049 | 1.000 | 1.000 | 0.079 | 1.000 | 0.010 | -0.185 | **0.006** | 0.688 | 0.013 |
| 7 | Medium | 0.077 | 0.452 | -0.142 | 0.077 | -0.452 | 0.154 | 1.000 | 0.518 | 0.003 | **0.006** | 0.688 | 0.016 |
| 8 | Medium | 1.000 | 0.053 | -0.368 | 0.053 | 0.492 | 0.031 | N/A | N/A | N/A | **0.006** | 0.688 | 0.015 |
| 9 | Medium | 0.147 | -0.374 | -0.697 | 0.147 | 0.374 | 0.697 | N/A | N/A | N/A | **0.006** | 0.688 | 0.016 |
| 10 | Old | **0.010** | 0.649 | 0.068 | 1.000 | 0.198 | -0.540 | 1.000 | 0.260 | -0.078 | **0.016** | 0.610 | 0.013 |
| 11 | Old | 0.872 | 0.059 | 0.235 | 0.872 | 0.059 | -0.117 | 0.747 | -0.098 | 0.134 | **0.010** | 0.649 | 0.011 |
| 12 | Old | 0.260 | -0.295 | -0.111 | 0.334 | 0.256 | 0.034 | 1.000 | -0.020 | 0.012 | **0.010** | 0.649 | 0.012 |
| 13 | Old | 0.260 | 0.295 | 0.421 | 0.520 | -0.177 | -0.399 | 1.000 | 0.334 | -0.291 | **0.016** | 0.610 | 0.011 |
| 14 | Old | 0.334 | -0.256 | -0.133 | 0.260 | 0.295 | 0.275 | 0.077 | -0.452 | -0.069 | **0.010** | 0.649 | 0.012 |
| 15 | Old | 1.000 | 1.000 | 12.125 | 0.872 | 0.059 | -0.951 | 0.147 | -0.374 | -0.268 | **0.016** | 0.610 | 0.011 |
| 16 | Old | 0.107 | -0.413 | -0.643 | 1.000 | 0.107 | 7.255 | 1.000 | 0.421 | -0.180 | **0.010** | 0.649 | 0.013 |
| 17 | Old | 0.629 | -0.138 | -0.133 | 0.629 | 0.138 | 0.131 | 1.000 | 0.162 | -0.003 | **0.006** | 0.688 | 0.013 |
| Other | N/A | 1.000 | 0.872 | 31.090 | 1.000 | 0.020 | -4.096 | **0.002** | 0.767 | 0.619 | **0.010** | 0.649 | 0.011 |

## 3.3 Greening of the landscape

We found an overall greening trend over the entire study area ($\tau = 0.65$, $p = 0.01$, NDVI increase of 0.01 $yr^{-1}$) and within all basins, except for the young basin, which showed a slight increase with no significant change ($p = 0.077$, $\tau = 0.45$, ***Table 2***). We also found that the NDVI trend with respect to basin age is spatially variable with faster rates of greening in medium basins than old or "other". Both wet and dry vegetation communities significantly increased in NDVI as well ($\tau = 0.65$, $p = 0.01$ for both wet and dry communities). The rate of increase in NDVI was faster for wet communities ($0.013 \pm 0.003$ $yr^{-1}$) than for dry communities ($0.011 \pm 0.002$ $yr^{-1}$). Pixel level analysis showed similar results to those aggregated by basins or vegetation. Wet areas

showed the largest change with rates of NDVI change around 0.05 to 0.08 $y^{-1}$. Dry ridges show NDVI changes closer to 0.01 to 0.04 $y^{-1}$ (***Figure 4***).

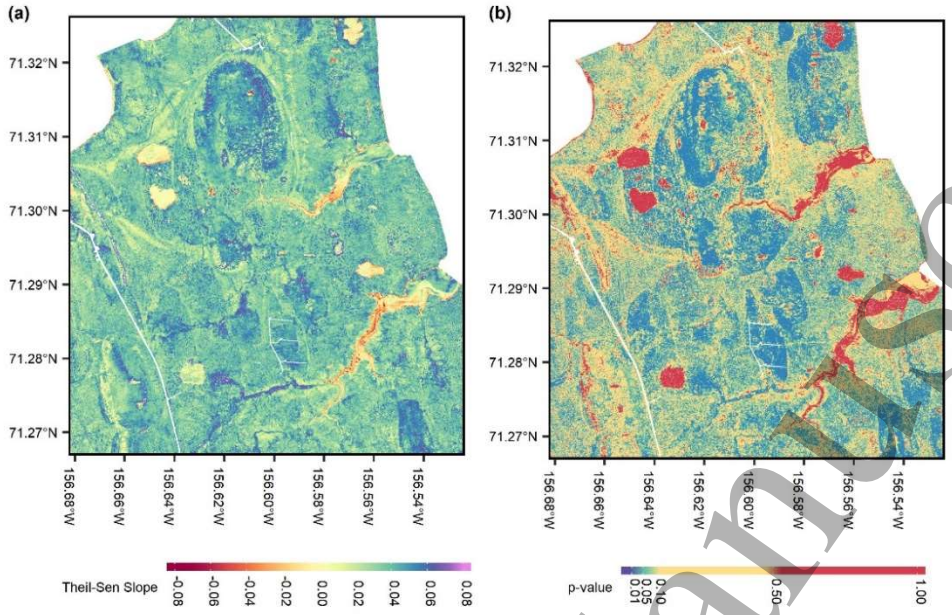


***Figure 4***: Pixel level change maps of the study area from 2002 to 2016. **(a)** The Theil-Sen slope estimate shows the largest changes came from water tracks in the south and basins 3, 4, 6 and 9. These areas had two to three times the rate of change of drier ridges around the same water tracks and surrounding basin 3, 4, and 11. Values are the NDVI change per year. **(b)** Mann-Kendall *p-values* show areas with significant changes were also largely located in wet areas including basins and water paths. Open water that was included in the analysis was the least significant and changed the least giving us confidence the observed changes were not due to sensor drift or artificial interferences.

### *3.3.1 NDVI controls*

TDD had the strongest correlation with NDVI (***Figure 5***, $F = 21.5$, $p < 0.001$, $R^2_m = 0.56$, $R^2_c = 0.77$, NDVI increase of $0.004 \pm 0.001$ $day^{-1}$) and explained most of the variability (the full multivariate model was not significantly different from the individual model of TDD ($p = 0.88$, likelihood ratio = 0.25)). GDD also strongly correlated with NDVI, with a slightly lower correlation coefficient than TDD ($F = 20.7$, $p < 0.001$, $R^2_m = 0.52$, $R^2_c = 0.77$, NDVI increase of $0.0008 \pm 0.0002$ $°C^{-1}$). As GDD was strongly collinear with TDD, they were not assessed together in any model ($F = 74.7$, $p < 0.001$, $R^2 = 0.84$). Mean growing season air temperature and VPD were not correlated to NDVI ($F = 1.2$, $p = 0.27$ for air temperature and $F = 0.53$, $p = 0.45$ for VPD). The first day of the year with a mean air temperature above freezing (i.e., first TDD) significantly shifted towards an earlier date at a rate of 1.07 days per year ($\tau = -0.47$, $p = 0.02$) but we found no evidence for changes in the last day above freezing ($\tau = -0.01$, $p = 1$).

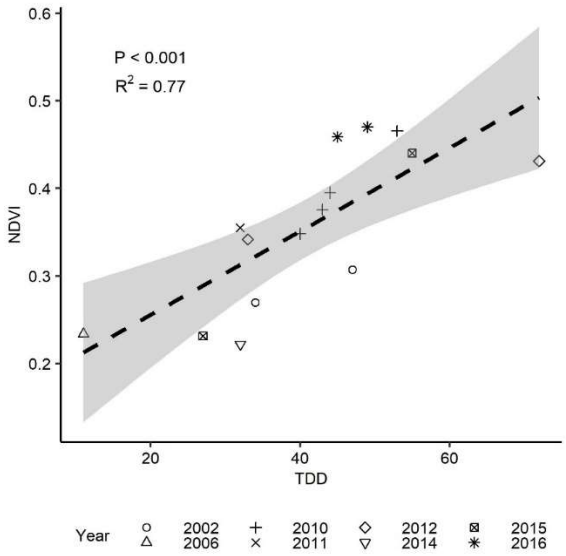


***Figure 5:*** NDVI as a function of thawing degree days (TDD) across all images showing as the growing season length increases, NDVI increases. As both NDVI and thawing degree days increased significantly over the course of the study, both were detrended in the LME testing the significance ($p < 0.001$, $R^2_m = 0.56$, $R^2_c = 0.77$, $N = 15$). Year was kept as a random continuous variable with NDVI and TDD as fixed variables.

# 4. Discussion

## 4.1 Vegetation community characteristics

Vegetation community groupings based on functional differences in carbon cycling characteristics (Treat et al., 2018, Davidson et al., 2016b, Sturtevant and Oechel, 2013), proved to be spectrally separable agreeing with prior studies (Lin et al., 2012, Davidson et al., 2016a). We were able to obtain ecological separation between vegetation communities as well using surveys of plant types (e.g. graminoid, moss, lichen, etc.).

Soil moisture content was the main environmental factor driving the separation of the vegetation communities and dictating their geographical distribution. Our results agree with findings from past studies (Lin et al., 2012) that showed vegetation communities near Utqiaġvik exist across a moisture gradient. Canopy heights differed between communities, with taller vegetation in wet communities and shorter vegetation in dry communities; canopy height has been used as a correlative metric for predicting above ground biomass in Arctic ecosystems (Berner et al., 2018). This suggests that wet communities typically have higher biomass than dry communities and therefore the relationship between biomass and moisture may exist as well (see supplementary material). Thaw depth did not differ between communities but this does not necessarily imply equal carbon storage in the active layer beneath the vegetation due to usually higher concentrations of organic matter in wetter lowlands, i.e. higher biomass given equal soil volume (Ping et al., 2008).

### 4.2 Vegetation community shifts at the landscape scale

We observed no shift in the overall cover of vegetation communities over the 14-year study. Measured shifts were around 1% and could be due to differences in water table, other seasonal differences, or classification errors. These results are in line with prior long-term studies of vegetation communities in this area showing 3% change over 60 years (1948 – 2008) when using high spatial resolution photography with satellite imagery (Lin et al., 2012). However, Lin et al. (2012) used four single images (1948, 1955, 1979 and 2008) to assess vegetation community change in their study which, did not account for intra-annual variability in standing water, a possible source of error. The seasonal progression in our data during 2010, where four images were acquired over two weeks (July 21 – Aug 3), showed a seasonal drying. Changes in surface water during the season can erroneously translate into error in predicted cover of vegetation communities by the random forest model. This result highlights the importance of considering timing of acquisition of high spatial resolution imagery in analyzing interannual patterns and change over long timescales.

Vegetation changes were observed in more localized areas. The young basin vegetation communities did not change and consisted mostly of wet vegetation. Old basins, comprised largely of low center polygons, are thawing where ice wedge degradation occurs over time scales ~60 years; the stage of degradation determines the degree to which the landscape is wet or dry (Liljedahl et al., 2016). We saw no overall significant changes in vegetation communities through the time-series but that does not mean degradation and shifts are not occurring. Polygon degradation effects could balance out if multiple stages are occurring simultaneously over the entire study area. According to our results, most changes occurred in medium and old age basins where medium age basins gained wet and lost dry communities and old age basins showed the opposite process (***Table 2, Figure 3***). Polygon degradation (Liljedahl et al., 2016) in old basins could increase drainage to the lowest part of the nearby landscape, medium basins, due to interconnected troughs and could explain increases in wetness in these medium basins. This is supported by the change map showing the wetting in these medium basins and drying along the edges (***Figure 3a***). This is also supported by the fact that medium basins had the lowest elevations (***Figure 1b***). Evidence of erosion or rising water levels exists where edges of water paths have gains in wet communities and edges of larger tributaries show dry vegetation to open water transitions (***Figure 3b***). These results suggest that even though total vegetation community compositions have not changed over the entire study area, high spatial resolution imagery allows us to detect localized but relatively balanced shifts.

### 4.3 Greening of the landscape

*4.3.1 Landscape Scale Greening Trends*

We found evidence of greening across vegetation communities and basins. Mean NDVI values of the whole image, split by vegetation type, basin age, and individual basins, displayed significant increasing trends in NDVI in all areas except the young basin. However, the young basin already had a relatively high NDVI (0.6 in 2016) and is at or above observed peaks for this ecosystem (Bhatt et al., 2017, May et al., 2017). Increases in NDVI can be due to changes in land cover type (Elmendorf et al., 2012) or increased vegetation biomass (Hudson and Henry, 2009).

Due to the lack of change in total vegetation community composition, we suggest that the most likely explanation for the observed greening in this ecosystem is increased plant productivity and growth.

*4.3.2 Vegetation Community Specific Greening Rates*

Our results show vegetation communities greening at different rates, in agreement with prior studies (Andresen et al., 2018, May et al., 2017). This trend has been locally shown to stand across the North Slope of Alaska where wet communities green faster under warming (May et al., 2017). Further, at a species level, wet communities have been observed to shift more than dry communities in this region over time, with sedge species replacing bryophytes (Villarreal et al., 2012), which could aid in NDVI increases. When trends for each pixel were analyzed, spatial patterns became even more evident (***Figure 4***). Some wet areas including many medium age basins (basins 2, 4, 6 and 9) and lower lying water paths had some of the highest rates of greening, sometimes more than double that of dry ridges (***Figure 4***). The *p*-value map also supported that these same areas have more instances significant change. The faster green up in wet areas confirms studies that show increases in moisture, expected in this region under climate predictions (Zhang et al., 2012), can enhance greening. Increases in moisture do not universally increase NDVI as shown in Raynolds and Walker (2016), where standing water depressed NDVI due to differential absorption of NIR and red irradiance by water. Lara et al. (2018) further showed negative correlations between precipitation and NDVI.

*4.3.3. NDVI controls and growing season length*

Greening was most correlated to increases in TDD, agreeing with previous studies (Huemmrich et al., 2010, Zeng et al., 2011). This further suggests that NDVI is most influenced by the thawing date (Andresen et al., 2018, Oberbauer et al., 2013); however, this may not always be true. If there is a freezing day after initial thaw, an early thawing can have the opposite effect on growth (Oberbauer et al., 2013), which causes browning (Phoenix and Bjerke, 2016). Mean temperature and VPD did not influence NDVI in our study, possibly because temperature and VPD have been shown to correlate with max NDVI (Bhatt et al., 2017, Bhatt et al., 2014, Epstein et al., 2012) which we were are unable to calculate with limited image acquisitions. Further, the temperature-NDVI relationship has been seen to weaken recently in the Arctic (Piao et al., 2014).

Many larger scale and coarser resolution studies have used the summer warmth index (SWI), the sum of mean monthly temperatures(Jia et al., 2003), to explain NDVI trends (Berner et al., 2018, Bhatt et al., 2013, Bhatt et al., 2017, Bhatt et al., 2010, Bhatt et al., 2014, Bieniek et al., 2015). SWI works for coarse-scale pan-Arctic studies that use maximum or time-integrated NDVI and have one value that represents the full growing season. However, in high spatial resolution investigations such as our study, a metric like TDD, that's measured on the acquisition date will better explain NDVI. Due to the tie between TDD and NDVI, we suggest that for high Arctic communities, if thawing continues to start earlier, then continued increases in NDVI are expected.

NDVI and vegetation communities differed seasonally in 2010 when four images were acquired within two weeks. This emphasizes that temporal and spatial events may greatly affect NDVI

values observed. We accounted for this by only using images acquired closer to peak growing season. While intraannual variability was observed in NDVI, the relationship with TDD, which also increased over the study period, gives us confidence in the overall greening trend. Further, these multiple images were used in time series analyses including the variability in trend analysis. Ultimately more satellite tasking and image acquisitions would be ideal to continue monitoring this trend. More meteorological data, such as precipitation and evapotranspiration would be ideal to tease out larger scale influences on NDVI (Andresen and Lougheed, 2015). Unfortunately, these datasets are not always available over longer time-series or spatial domains, especially within remote areas like the Arctic.

## 5. Conclusion

We found evidence of greening across the landscape, particularly in wet areas, and a balanced shift in vegetation communities. TDD was best correlated to the positive greening signal. There was no large shift in vegetation community assemblage, but localized changes were observed showing spatially variable wetting and drying. Our study emphasizes the increased ability of high-resolution remote sensing to analyze details in change detection analyses in the Arctic. Specifically, we were able to observe that wet communities may respond to warming at a faster rate than drier communities.

Our study analyzes a small area in the Arctic but takes a detailed approach to understanding Arctic greening. Many studies have looked at large scale changes which are important in a global context but lack detailed explanations (Myers-Smith et al., 2019). Only by understanding drivers of greening can we more accurately predict future vegetation productivity in the Arctic, which is currently of great importance given that experts cannot currently agree on the direction of change of the carbon balance (Abbott et al., 2016).

## Acknowledgements

This work was funded by the National Science Foundation (NSF) Office of Polar Programs (OPP) awarded to DZ and WCO (award number 1204263, and 1702797) with additional logistical support funded by the NSF Office of Polar Programs, by the NASA ABoVE Program (NNX16AF94A) awarded to WCO and DZ, by NOAA EPP (award number NA16SEC4810008) to WCO, from the European Union's Horizon 2020 research and innovation program under grant agreement No. 629727890 to WCO and DZ, and from the Natural Environment Research Council (NERC) UAMS Grant (NE/P002552/1) to WCO and DZ. We thank NOAA/ESRL for the meteorological data which is provided by NOAA/ESRL BRW from their website https://www.esrl.noaa.gov/gmd/obop/brw/. The data that support the findings of this study are openly available at DOI. Geospatial support for this work provided by the Polar Geospatial Center under NSF OPP award 1204263, and 1702797. This research was conducted on land owned by the Ukpeaġvik Inupiat Corporation (UIC) whom we thank for their support. Authors also thank the R developing team (R core team, Vienna, Austria) in creating the open source R statistical software. The data that support the findings in this study are openly available.

## References:


Abbott, B. W., Jones, J. B., Schuur, E. a. G., Chapin Iii, F. S., Bowden, W. B., Bret-Harte, M. S., Epstein, H. E., Flannigan, M. D., Harms, T. K., Hollingsworth, T. N., Mack, M. C., Mcguire, A. D., Natali, S. M., Rocha, A. V., Tank, S. E., Turetsky, M. R., Vonk, J. E., Wickland, K. P., Aiken, G. R., Alexander, H. D., Amon, R. M. W., Benscoter, B. W., Bergeron, Y., Bishop, K., Blarquez, O., Ben, B.-L., Breen, A. L., Buffam, I., Cai, Y., Carcaillet, C., Carey, S. K., Chen, J. M., Chen, H. Y. H., Christensen, T. R., Cooper, L. W., Cornelissen, J. H. C., De Groot, W. J., Deluca, T. H., Dorrepaal, E., Fetcher, N., Finlay, J. C., Forbes, B. C., French, N. H. F., Gauthier, S., Girardin, M. P., Goetz, S. J., Goldammer, J. G., Gough, L., Grogan, P., Guo, L., Higuera, P. E., Hinzman, L., Hu, F. S., Hugelius, G., Jafarov, E. E., Jandt, R., Johnstone, J. F., Jan, K., Kasischke, E. S., Kattner, G., Kelly, R., Keuper, F., Kling, G. W., Kortelainen, P., Kouki, J., Kuhry, P., Laudon, H., Laurion, I., Macdonald, R. W., Mann, P. J., Martikainen, P. J., Mcclelland, J. W., Molau, U., Oberbauer, S. F., Olefeldt, D., Paré, D., Parisien, M.-A., Payette, S., Peng, C., Pokrovsky, O. S., Rastetter, E. B., Raymond, P. A., Raynolds, M. K., Rein, G., Reynolds, J. F., Robards, M., Rogers, B. M., Schädel, C., Schaefer, K., Schmidt, I. K., Shvidenko, A., Sky, J., Spencer, R. G. M., Starr, G., Striegl, R. G., Teisserenc, R., Tranvik, L. J., Virtanen, T., Welker, J. M. & Zimov, S. 2016. Biomass offsets little or none of permafrost carbon release from soils, streams, and wildfire: an expert assessment. *Environmental Research Letters,* 11.

Andresen, C. G. & Lougheed, V. L. 2015. Disappearing Arctic tundra ponds: Fine-scale analysis of surface hydrology in drained thaw lake basins over a 65 year period (1948-2013). *Journal of Geophysical Research: Biogeosciences,* 120**,** 466-479.

Andresen, C. G., Tweedie, C. E. & Lougheed, V. L. 2018. Climate and nutrient effects on Arctic wetland plant phenology observed from phenocams. *Remote Sensing of Environment,* 205**,** 46-55.

Barton, K. 2018. MuMIn: Multi-Model Inference.

Bartsch, A., Höfler, A., Kroisleitner, C. & Trofaier, A. 2016. Land Cover Mapping in Northern High Latitude Permafrost Regions with Satellite Data: Achievements and Remaining Challenges. *Remote Sensing,* 8.

Berner, L. T., Jantz, P., Tape, K. D. & Goetz, S. J. 2018. Tundra plant above-ground biomass and shrub dominance mapped across the North Slope of Alaska. *Environmental Research Letters,* 13.

Bhatt, U. S., Walker, D. A., Raynolds, M., Bieniek, P., Epstein, H., Comiso, J., Pinzon, J., Tucker, C. & Polyakov, I. 2013. Recent Declines in Warming and Vegetation Greening Trends over Pan-Arctic Tundra. *Remote Sensing,* 5**,** 4229-4254.

Bhatt, U. S., Walker, D. A., Raynolds, M. K., Bieniek, P. A., Epstein, H. E., Comiso, J. C., Pinzon, J. E., Tucker, C. J., Steele, M., Ermold, W. & Zhang, J. 2017. Changing seasonality of panarctic tundra vegetation in relationship to climatic variables. *Environmental Research Letters,* 12.

Bhatt, U. S., Walker, D. A., Raynolds, M. K., Comiso, J. C., Epstein, H. E., Jia, G., Gens, R., Pinzon, J. E., Tucker, C. J., Tweedie, C. E. & Webber, P. J. 2010. Circumpolar Arctic Tundra Vegetation Change Is Linked to Sea Ice Decline. *Earth Interactions,* 14**,** 1-20.

Bhatt, U. S., Walker, D. A., Walsh, J. E., Carmack, E. C., Frey, K. E., Meier, W. N., Moore, S. E., Parmentier, F.-J. W., Post, E., Romanovsky, V. E. & Simpson, W. R. 2014. Implications of Arctic Sea Ice Decline for the Earth System. *Annual Review of Environment and Resources,* 39**,** 57-89.

Bieniek, P. A., Bhatt, U. S., Walker, D. A., Raynolds, M. K., Comiso, J. C., Epstein, H. E., Pinzon, J. E., Tucker, C. J., Thoman, R. L., Tran, H., Mölders, N., Steele, M., Zhang, J. & Ermold, W. 2015. Climate Drivers Linked to Changing Seasonality of Alaska Coastal Tundra Vegetation Productivity. *Earth Interactions,* 19**,** 1-29.

Billings, W. D. & Peterson, K. M. 1980. Vegetational Change and Ice-Wedge Polygons through the Thaw-Lake Cycle in Arctic Alaska. *Arctic and Alpine Research,* 12**,** 413-432.

Bronaugh, D. & Werner, A. 2019. zyp: Zhang + Yue-Pilon Trends Package.

Chapin, F. S., 3rd, Sturm, M., Serreze, M. C., Mcfadden, J. P., Key, J. R., Lloyd, A. H., Mcguire, A. D., Rupp, T. S., Lynch, A. H., Schimel, J. P., Beringer, J., Chapman, W. L., Epstein, H. E., Euskirchen, E. S., Hinzman, L. D., Jia, G., Ping, C. L., Tape, K. D., Thompson, C. D., Walker, D. A. & Welker, J. M. 2005. Role of land-surface changes in arctic summer warming. *Science,* 310**,** 657-60.

Chapman, D. S., Bonn, A., Kunin, W. E. & Cornell, S. J. 2009. Random Forest characterization of upland vegetation and management burning from aerial imagery. *Journal of Biogeography,* 37**,** 37-46.

Davidson, S. J., Santos, M. J., Sloan, V. L., Watts, J. D., Phoenix, G. K., Oechel, W. C. & Zona, D. 2016a. Mapping Arctic Tundra Vegetation Communities Using Field Spectroscopy and Multispectral Satellite Data in North Alaska, USA. *Remote Sensing,* 8.

Davidson, S. J., Sloan, V. L., Phoenix, G. K., Wagner, R., Fisher, J. P., Oechel, W. C. & Zona, D. 2016b. Vegetation Type Dominates the Spatial Variability in CH4 Emissions Across Multiple Arctic Tundra Landscapes. *Ecosystems,* 19**,** 1116-1132.

Elmendorf, S. C., Henry, G. H., Hollister, R. D., Bjork, R. G., Bjorkman, A. D., Callaghan, T. V., Collier, L. S., Cooper, E. J., Cornelissen, J. H., Day, T. A., Fosaa, A. M., Gould, W. A., Gretarsdottir, J., Harte, J., Hermanutz, L., Hik, D. S., Hofgaard, A., Jarrad, F., Jonsdottir, I. S., Keuper, F., Klanderud, K., Klein, J. A., Koh, S., Kudo, G., Lang, S. I., Loewen, V., May, J. L., Mercado, J., Michelsen, A., Molau, U., Myers-Smith, I. H., Oberbauer, S. F., Pieper, S., Post, E., Rixen, C., Robinson, C. H., Schmidt, N. M., Shaver, G. R., Stenstrom, A., Tolvanen, A., Totland, O., Troxler, T., Wahren, C. H., Webber, P. J., Welker, J. M. & Wookey, P. A. 2012. Global assessment of experimental climate warming on tundra vegetation: heterogeneity over space and time. *Ecol Lett,* 15**,** 164-75.

Epstein, H. E., Raynolds, M. K., Walker, D. A., Bhatt, U. S., Tucker, C. J. & Pinzon, J. E. 2012. Dynamics of aboveground phytomass of the circumpolar Arctic tundra during the past three decades. *Environmental Research Letters,* 7.

Evans, J. S. 2018. spatialEco.

Fernandes, R. & Leblanc, G. S. 2005. Parametric (modified least squares) and non-parametric (Theil–Sen) linear regressions for predicting biophysical parameters in the presence of measurement errors. *Remote Sensing of Environment,* 95**,** 303-316.

Forbes, B. C., Macias-Fauria, M. & Zetterberg, P. 2010. Russian Arctic warming and 'greening' are closely tracked by tundra shrub willows. *Global Change Biology,* 16**,** 1542-1554.

Frost, G. V., Epstein, H. E. & Walker, D. A. 2014. Regional and landscape-scale variability of Landsat-observed vegetation dynamics in northwest Siberian tundra. *Environmental Research Letters,* 9.

Gandhi, G. M., Parthiban, S., Thummalu, N. & Christy, A. 2015. Ndvi: Vegetation Change Detection Using Remote Sensing and Gis – A Case Study of Vellore District. *Procedia Computer Science,* 57**,** 1199-1210.

Goetz, S. J., Bunn, A. G., Fiske, G. J. & Houghton, R. A. 2005. Satellite-observed photosynthetic trends across boreal North America associated with climate and fire disturbance. *Proceedings of the National Academy of Sciences of the United States of America,* 102**,** 13521-13525.

Hinkel, K. M., Eisner, W. R., Bockheim, J. G., Nelson, F. E., Peterson, K. M. & Dai, X. 2003. Spatial Extent, Age, and Carbon Stocks in Drained Thaw Lake Basins on the Barrow Peninsula, Alaska. *Arctic, Antarctic, and Alpine Research,* 35**,** 291-300.

Hudson, J. M. G. & Henry, G. H. R. 2009. Increased plant biomass in a High Arctic heath community from 1981 to 2008. *Ecology,* 90**,** 2657-2663.

Huemmrich, K. F., Kinoshita, G., Gamon, J. A., Houston, S., Kwon, H. & Oechel, W. C. 2010. Tundra carbon balance under varying temperature and moisture regimes. *Journal of Geophysical Research,* 115.

Hugelius, G., Strauss, J., Zubrzycki, S., Harden, J. W., Schuur, E. a. G., Ping, C. L., Schirrmeister, L., Grosse, G., Michaelson, G. J., Koven, C. D., O'donnell, J. A., Elberling, B., Mishra, U., Camill, P., Yu, Z., Palmtag, J. & Kuhry, P. 2014. Estimated stocks of circumpolar permafrost carbon with quantified uncertainty ranges and identified data gaps. *Biogeosciences,* 11**,** 6573-6593.

Ipcc 2013. Climate Change 2013: The Physical Science Basis. Contribution of Working Group I to the Fifth Assessment Report of the Intergovernmental Panel on Climate Change. *In:* Stocker, T. F., D. Qin, G.-K. Plattner, M. Tignor, S.K. Allen, J. Boschung, A. Nauels, Y. Xia, V. Bex and P.M. Midgley (ed.). United Kingdom and New York, NY, USA.

Jia, G. J., Epstein, H. E. & Walker, D. A. 2003. Greening of arctic Alaska, 1981–2001. *Geophysical Research Letters,* 30.

Joos, F., Prentice, I. C., Sitch, S., Meyer, R., Hooss, G., Plattner, G.-K., Gerber, S. & Hasselmann, K. 2001. Global warming feedbacks on terrestrial carbon uptake under the Intergovernmental Panel on Climate Change (IPCC) Emission Scenarios. *Global Biogeochemical Cycles,* 15**,** 891-907.

Kauth, R. J. & Thomas, G. The tasselled cap--a graphic description of the spectral-temporal development of agricultural crops as seen by Landsat. LARS symposia, 1976. 159.

Lara, M. J., Nitze, I., Grosse, G., Martin, P. & Mcguire, A. D. 2018. Reduced arctic tundra productivity linked with landform and climate change interactions. *Sci Rep,* 8**,** 2345.

Liljedahl, A. K., Boike, J., Daanen, R. P., Fedorov, A. N., Frost, G. V., Grosse, G., Hinzman, L. D., Iijma, Y., Jorgenson, J. C., Matveyeva, N., Necsoiu, M., Raynolds, M. K., Romanovsky, V. E., Schulla, J., Tape, K. D., Walker, D. A., Wilson, C. J., Yabuki, H. & Zona, D. 2016. Pan-Arctic ice-wedge degradation in warming permafrost and its influence on tundra hydrology. *Nature Geoscience,* 9**,** 312-318.

Lin, D. H., Johnson, D. R., Andresen, C. G. & Tweedie, C. E. 2012. High spatial resolution decade-time scale land cover change at multiple locations in the Beringian Arctic (1948–2000s). *Environmental Research Letters,* 7.

Macias-Fauria, M., Karlsen, S. R. & Forbes, B. C. 2017. Disentangling the coupling between sea ice and tundra productivity in Svalbard. *Sci Rep,* 7**,** 8586.

May, J., Healey, N., Ahrends, H., Hollister, R., Tweedie, C., Welker, J., Gould, W. & Oberbauer, S. 2017. Short-Term Impacts of the Air Temperature on Greening and Senescence in Alaskan Arctic Plant Tundra Habitats. *Remote Sensing,* 9.

Mishra, U. & Riley, W. J. 2012. Alaskan soil carbon stocks: spatial variability and dependence on environmental factors. *Biogeosciences,* 9**,** 3637-3645.

Myers-Smith, I., Forbes, B. C., Wilmking, M., Hallinger, M., Lantz, T., Blok, D., Tape, K. D., Macias-Fauria, M., Sass-Klaassen, U., Lévesque, E., Boudreau, S., Ropars, P., Hermanutz, L., Trant, A., Collier, L. S., Weijers, S., Rozema, J., Rayback, S. A., Schmidt, N. M., Schaepman-Strub, G., Wipf, S., Rixen, C., Ménard, C. B., Venn, S., Goetz, S., Andreu-Hayles, L., Elmendorf, S., Ravolainen, V., Welker, J., Grogan, P., Epstein, H. E. & Hik, D. S. 2011. Shrub expansion in tundra ecosystems: dynamics, impacts and research priorities. *Environmental Research Letters,* 6.

Myers-Smith, I., Kerby, J. T., Phoenix, G. K., Bjerke, J., Epstein, H. E., Assmann, J., John, C., Andreu-Hayles, L., Angers-Blodin, S., Beck, P. S. A., Berner, L. T., Bhatt, U. S., Bjorkman, A., Blok, D., Bryn, A., Christiansen, C. T., Cornelissen, J. H. C., Cunliffe, A. M., Elmendorf, S. C., Forbes, B. C., Goetz, S. J., Hollister, R. D., Jong, R. D., Loranty, M., Macias-Fauria, M., Maseyk, K., Normand, S., Olofsson, J., Parker, T. C., Parmentier, F.-J. W., Post, E. S., Schaepman-Strub, G., Stordal, F., Sullivan, P., Thomas, H. J. D., Tømmervik, H., Treharne, R., Tweedie, C. E., Walker, D. A., Wilmking, M. & Wipf, S. 2019. Complexity Revealed in the Greening of the Arctic. *EcoEvoRxiv*.

Natali, S. M., Schuur, E. a. G., Mauritz, M., Schade, J. D., Celis, G., Crummer, K. G., Johnston, C., Krapek, J., Pegoraro, E., Salmon, V. G. & Webb, E. E. 2015. Permafrost thaw and soil moisture driving

CO2 and CH4 release from upland tundra. *Journal of Geophysical Research: Biogeosciences,* 120**,** 525-537.

Nitze, I. & Grosse, G. 2016. Detection of landscape dynamics in the Arctic Lena Delta with temporally dense Landsat time-series stacks. *Remote Sensing of Environment,* 181**,** 27-41.

Oberbauer, S. F., Elmendorf, S. C., Troxler, T. G., Hollister, R. D., Rocha, A. V., Bret-Harte, M. S., Dawes, M. A., Fosaa, A. M., Henry, G. H., Hoye, T. T., Jarrad, F. C., Jonsdottir, I. S., Klanderud, K., Klein, J. A., Molau, U., Rixen, C., Schmidt, N. M., Shaver, G. R., Slider, R. T., Totland, O., Wahren, C. H. & Welker, J. M. 2013. Phenological response of tundra plants to background climate variation tested using the International Tundra Experiment. *Philos Trans R Soc Lond B Biol Sci,* 368**,** 20120481.

Oksanen, J., Blanchet, G. F., Friendly, M., Kindt, R., Legendre, P., Mcglinn, D., Minchin, P. R., O'hara, R. B., Simpson, G. L., Solymos, P., Stevens, M. H. H., Szoecs, E. & Wagner, H. 2018. vegan: Community Ecology Package.

Phoenix, G. K. & Bjerke, J. W. 2016. Arctic browning: extreme events and trends reversing arctic greening. *Glob Chang Biol,* 22**,** 2960-2.

Piao, S., Nan, H., Huntingford, C., Ciais, P., Friedlingstein, P., Sitch, S., Peng, S., Ahlstrom, A., Canadell, J. G., Cong, N., Levis, S., Levy, P. E., Liu, L., Lomas, M. R., Mao, J., Myneni, R. B., Peylin, P., Poulter, B., Shi, X., Yin, G., Viovy, N., Wang, T., Wang, X., Zaehle, S., Zeng, N., Zeng, Z. & Chen, A. 2014. Evidence for a weakening relationship between interannual temperature variability and northern vegetation activity. *Nat Commun,* 5**,** 5018.

Ping, C.-L., Michaelson, G. J., Jorgenson, M. T., Kimble, J. M., Epstein, H., Romanovsky, V. E. & Walker, D. A. 2008. High stocks of soil organic carbon in the North American Arctic region. *Nature Geoscience,* 1**,** 615-619.

Pinheiro, J., Bates, D., Debroy, S., Sarkar, D. & Team, R. C. 2018. nlme: Linear and Nonlinear Mixed Effects Models.

Price, D. T., Alfaro, R. I., Brown, K. J., Flannigan, M. D., Fleming, R. A., Hogg, E. H., Girardin, M. P., Lakusta, T., Johnston, M., Mckenney, D. W., Pedlar, J. H., Stratton, T., Sturrock, R. N., Thompson, I. D., Trofymow, J. A. & Venier, L. A. 2013. Anticipating the consequences of climate change for Canada's boreal forest ecosystems. *Environmental Reviews,* 21**,** 322-365.

R Core Team 2018. R: A Language and Environment for Statistical Computing.

Raynolds, M. K. & Walker, D. A. 2016. Increased wetness confounds Landsat-derived NDVI trends in the central Alaska North Slope region, 1985–2011. *Environmental Research Letters,* 11.

Raynolds, M. K., Walker, D. A., Epstein, H. E., Pinzon, J. E. & Tucker, C. J. 2011. A new estimate of tundra-biome phytomass from trans-Arctic field data and AVHRR NDVI. *Remote Sensing Letters,* 3**,** 403-411.

Romanovsky, V., Smith, S. L., Shiklomanov, N., Streletskiy, D. A., Isaken, K., Kholodov, A. L., Christensen, H. H., Drozdov, D. S., Malkova, G. V. & Marchenko, S. 2017. [The Arctic] terrestrial permafrost [in "State ofthe Climate in 2016"] State ofthe Climate in 2016. *Bulletin of the American Meteorological Society,* 98.

Schuur, E. A., Abbott, B. W., Bowden, W. B., Brovkin, V., Camill, P., Canadell, J. G., Chanton, J. P., Chapin, F. S., Christensen, T. R., Ciais, P., Crosby, B. T., Czimczik, C. I., Grosse, G., Harden, J., Hayes, D. J., Hugelius, G., Jastrow, J. D., Jones, J. B., Kleinen, T., Koven, C. D., Krinner, G., Kuhry, P., Lawrence, D. M., Mcguire, A. D., Natali, S. M., O'donnell, J. A., Ping, C. L., Riley, W. J., Rinke, A., Romanovsky, V. E., Sannel, A. B. K., Schädel, C., Schaefer, K., Sky, J., Subin, Z. M., Tarnocai, C., Turetsky, M. R., Waldrop, M. P., Walter Anthony, K. M., Wickland, K. P., Wilson, C. J. & Zimov, S. A. 2013. Expert assessment of vulnerability of permafrost carbon to climate change. *Climatic Change,* 119**,** 359-374.

Schuur, E. A., Mcguire, A. D., Schadel, C., Grosse, G., Harden, J. W., Hayes, D. J., Hugelius, G., Koven, C. D., Kuhry, P., Lawrence, D. M., Natali, S. M., Olefeldt, D., Romanovsky, V. E., Schaefer, K., Turetsky, M. R., Treat, C. C. & Vonk, J. E. 2015. Climate change and the permafrost carbon feedback. *Nature,* 520**,** 171-9.

Sen, P. K. 1968. Estimates of the Regression Coefficient Based on Kendall's Tau. *Journal of the American Statistical Association,* 63**,** 1379-1389.

Serreze, M. C. & Francis, J. A. 2006. The Arctic Amplification Debate. *Climatic Change,* 76**,** 241-264.

Spencer, R. G. M., Mann, P. J., Dittmar, T., Eglinton, T. I., Mcintyre, C., Holmes, R. M., Zimov, N. & Stubbins, A. 2015. Detecting the signature of permafrost thaw in Arctic rivers. *Geophysical Research Letters,* 42**,** 2830-2835.

Stow, D. A., Hope, A., Mcguire, D., Verbyla, D., Gamon, J., Huemmrich, F., Houston, S., Racine, C., Sturm, M., Tape, K., Hinzman, L., Yoshikawa, K., Tweedie, C., Noyle, B., Silapaswan, C., Douglas, D., Griffith, B., Jia, G., Epstein, H., Walker, D. A., Daeschner, S., Petersen, A., Zhou, L. & Myneni, R. 2004. Remote sensing of vegetation and land-cover change in Arctic Tundra Ecosystems. *Remote Sensing of Environment,* 89**,** 281-308.

Sturtevant, C. S. & Oechel, W. C. 2013. Spatial variation in landscape-level CO2 and CH4 fluxes from arctic coastal tundra: influence from vegetation, wetness, and the thaw lake cycle. *Glob Chang Biol,* 19**,** 2853-66.

Suzuki, R., Nomaki, T. & Yasunari, T. 2001. Spatial distribution and its seasonality of satellite-derived vegetation index (NDVI) and climate in Siberia. *International Journal of Climatology,* 21**,** 1321-1335.

Tape, K. E. N., Sturm, M. & Racine, C. 2006. The evidence for shrub expansion in Northern Alaska and the Pan-Arctic. *Global Change Biology,* 12**,** 686-702.

Theil, H. 1992. A Rank-Invariant Method of Linear and Polynomial Regression Analysis. *In:* Raj, B. & Koerts, J. (eds.) *Henri Theil's Contributions to Economics and Econometrics: Econometric Theory and Methodology.* Dordrecht: Springer Netherlands.

Treat, C. C., Marushchak, M. E., Voigt, C., Zhang, Y., Tan, Z., Zhuang, Q., Virtanen, T. A., Rasanen, A., Biasi, C., Hugelius, G., Kaverin, D., Miller, P. A., Stendel, M., Romanovsky, V., Rivkin, F., Martikainen, P. J. & Shurpali, N. J. 2018. Tundra landscape heterogeneity, not interannual variability, controls the decadal regional carbon balance in the Western Russian Arctic. *Glob Chang Biol,* 24**,** 5188-5204.

Van Beijma, S., Comber, A. & Lamb, A. 2014. Random forest classification of salt marsh vegetation habitats using quad-polarimetric airborne SAR, elevation and optical RS data. *Remote Sensing of Environment,* 149**,** 118-129.

Villarreal, S., Hollister, R. D., Johnson, D. R., Lara, M. J., Webber, P. J. & Tweedie, C. E. 2012. Tundra vegetation change near Barrow, Alaska (1972–2010). *Environmental Research Letters,* 7.

Walker, D. A., Raynolds, M. K., Daniëls, F. J. A., Einarsson, E., Elvebakk, A., Gould, W. A., Katenin, A. E., Kholod, S. S., Markon, C. J., Melnikov, E. S., Moskalenko, N. G., Talbot, S. S., Yurtsev, B. A. & The Other Members of The, C. T. 2005. The Circumpolar Arctic vegetation map. *Journal of Vegetation Science,* 16**,** 267-282.

Webber, P. J. 1978. Spatial and Temporal Variation of the Vegetation and Its Production, Barrow, Alaska. *In:* Tieszen, L. L. (ed.) *Vegetation and Production Ecology of an Alaskan Arctic Tundra.* New York, NY: Springer New York.

Westergaard-Nielsen, A., Lund, M., Pedersen, S. H., Schmidt, N. M., Klosterman, S., Abermann, J. & Hansen, B. U. 2017. Transitions in high-Arctic vegetation growth patterns and ecosystem productivity tracked with automated cameras from 2000 to 2013. *Ambio,* 46**,** 39-52.

Wilson, C. J., Gangodagamage, C. & Rowland, J. 2013. Digital Elevation Model, 0.5 m, Barrow Environmental Observatory, Alaska, 2012. Next Generation Ecosystem Experiments Arctic Data Collection: Oak Ridge National Laboratory.

Yarbrough, L. D., Easson, G. & Kuszmaul, J. S. QuickBird 2 tasseled cap transform coefficients: a comparison of derivation methods. Pecora, 2005. 23-27.

Yue, S., Pilon, P., Phinney, B. & Cavadias, G. 2002. The influence of autocorrelation on the ability to detect trend in hydrological series. *Hydrological Processes,* 16**,** 1807-1829.

Zeng, H., Jia, G. & Epstein, H. 2011. Recent changes in phenology over the northern high latitudes detected from multi-satellite data. *Environmental Research Letters,* 6.

Zhang, X., He, J., Zhang, J., Polyakov, I., Gerdes, R., Inoue, J. & Wu, P. 2012. Enhanced poleward moisture transport and amplified northern high-latitude wetting trend. *Nature Climate Change,* 3**,** 47-51.

Zhang, X., Jayavelu, S., Liu, L., Friedl, M. A., Henebry, G. M., Liu, Y., Schaaf, C. B., Richardson, A. D. & Gray, J. 2018. Evaluation of land surface phenology from VIIRS data using time series of PhenoCam imagery. *Agricultural and Forest Meteorology,* 256-257**,** 137-149.